Distribution Category:
Advanced Reactor Safety
Research—Fast Reactors
(NRC-7)

ANL-76-13

ARGONNE NATIONAL LABORATORY
9700 South Cass Avenue
Argonne, Illinois 60439

PHYSICS OF REACTOR SAFETY

Quarterly Report
October—December 1975

Applied Physics Division

Work performed for the
Division of Reactor Safety Research
U. S. Nuclear Regulatory Commission

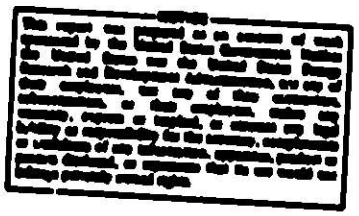

Previous reports in this series

ANL-75-31 January—March 1975
ANL-75-67 April—June 1975
ANL-76-6 July—September 1975

TABLE OF CONTENTS

LIST OF FIGURES

LIST OF TABLES

PHYSICS OF REACTOR SAFETY

Quarterly Report
October--December 1975

I. ABSTRACT

This quarterly progress report summarizes work done in Argonne National Laboratory's Applied Physics Division for the Division of Reactor Safety Research of the U. S. Nuclear Regulatory Commission during the months of October-December 1975. It includes reports on reactor safety research and technical coordination of the RSR safety analysis program by members of the Reactor Safety Appraisals Group, Monte Carlo analysis of safety-related critical assembly experiments by members of the Theoretical Fast Reactor Physics Group, and planning of DEMO safety-related critical experiments by members of the Zero Power Reactor (ZPR) Planning and Experiments Group.

TECHNICAL COORDINATION - FAST REACTOR SAFETY ANALYSIS (A2015)

II. SUMMARY

Further calculations of reactivity coefficients and power distribution have been carried out for the beginning-of-life (BOL) state for the CRBR, using a full-core-height R-Z model. Good agreement with values reported by WARD in the CRBR PSAR was found in almost all cases. Partially inserted control rods were found to skew the axial power shape between 16 and 31% for various locations. Axial skewing of power distribution due to sodium density and fuel temperature variations was found to be small. For voiding of all the core except control subassemblies, the Doppler -Tdk/dT is about 60% of the sodium-in value, voiding the control subassemblies reduces the inner-core value another 20%. -Tdk/dT is 9 to 15% higher for the range 1100°-2200°K. Axial skewing of reactivity coefficients was found to be quite sensitive to partial insertion of control rods.

The use of simple energy balances has given valuable insight into conditions for the stability of boiling fuel/steel pools. The potential pressure rise from transfer of heat from molten fuel to molten steel has been calculated as a function of initial temperature difference between fuel and steel and fuel/steel mass ratios to determine ranges of these parameters in which a pool pressurized from above could resist collapse through generation of steel vapor pressure.

A system for display of POOL program results on movie film has been developed, and a two minute demonstration film has been prepared showing the influence of heat transfer on the response of a boiling pool to uniform overpressure.

In order to be able to follow the behavior of molten pools of core material for long periods in recriticality studies, it has been necessary to try to develop a numerical hydrodynamics technique that combines separate treatment of the compressible and incompressible regions of the pool. Conventional compressible-flow techniques are too slow for this purpose. Each cell of the pool is examined to see if it is compressible or incompressible. In the former case, the current POOL algorithms are applied; in the latter case an incompressible-flow algorithm of Hirt et al and the particle-in-cell treatment of Harlow and Evans is applied. Problems have been encountered in applying this technique with both convergence and stability, and minor boundary-value problems have appeared, but none appears unsurmountable.

Debugging of the advanced FCI (fuel-coolant interaction) model has continued. It has been found necessary to resort to a marker particle and cell technique instead of using a continuous distribution of particles as orginally planned. It was also found necessary for stability reasons to assume instantaneous pressure equilibration between the failed part of a pin and the adjacent coolant channel rather than to compute an ejection velocity for fuel and gas based on pressure difference. Finite-difference numerical techniques being applied seem to be satisfactory so far, but the most severe conditions have not yet been applied.

Consultations have been held with personnel of Sandia Laboratory concerning equation-of-state measurements for UO_2 and use of the ACPR facility. Discussions were held with BNL and Licensing personnel regarding calculation of CRBR physics parameters, and with BNL personnel regarding the use of the DEMO code and development of the SSC code.

A number of papers have been presented relevant to ANL RSR-funded activities at the PSAR meeting at Albuquerque and the San Francisco ANS meeting.

III. STUDY OF BASIC PROBLEMS IN ACCIDENT ANALYSIS

A. Initiating Condition Variations

1. Power and Reactivity Distribution in the Clinch River Breeder Reactor at beginning-of-Life (BOL) (Kalimullah and H. H. Hummel)

We have summarized here results of continuing calculations of power, unvoided and voided Doppler coefficients, sodium void, and steel and core fuel worth distributions in the CRBR at BOL (with light water reactor grade plutonium fuel) to be used in hypothetical core disruptive accidents (HCDA) analysis for the review of the preliminary safety analysis report (PSAR).[1] Calculations of the effect of the use of Fast Flux Test Facility (FFTF) grade plutonium are not included here. The full-height hot full power r-z model used is based on $(U,Pu)O_2$ masses, dimensions and volume fractions reported in the PSAR[1] (Table D4-1), with the sodium density varying axially as a function of its steady state temperature calculated by the SAS Code.[2] The thicknesses of the axial and radial reflectors (40 cm and 20 cm) are essentially infinite. The central control rod and the 6 rods at flats of row 7 made of natural B_4C are 2/3 inserted. A 27-group region- and temperature-dependent, sodium present and

voided cross-section set was generated from the ENDF/B-III data using the MC^2-2 and SDX C[illegible] for these calculations:

a. Power distribution: With fuel assumed at a uniform temperature of 1100°K, the maximum (in row 7) and the minimum (in row 4) axial power shape skewness [(power density at core bottom)/(power density at core top) minus 1] are 31% and 16%, compared to 20% row-independent skewness reported in the PSAR.[1] Calculations with all control rods out indicate that the axial variation of sodium density causes an insignificant skewness (~0.2%). Axial variation of fuel temperature seems to have a greater effect (3 to 4%). Core subassembly radial power factors computed from a 2-D triangular mesh diffusion theory calculation with the central rod and the 6 rods at flats of row 7 fully inserted have been compared with those in the PSAR (Fig. 4.3-5). The present calculation gives slightly higher (maximum difference 1% in row 2) values in rows 2-6, and lower (maximum difference 1.[illegible]% at corners of row 9) in rows 7-9.

b. Doppler coefficient: Studies have been made of the effects on the spatial distribution of the Doppler coefficient of (a) a set of five stages of voiding from no voiding to no sodium present at all, (b) varying temperature ranges and (c) varying reflector thicknesses. Perturbation calculations with real and adjoint fluxes at each end of the temperature range were performed. Over the range 2200-4400°K (of interest in HCDA analysis) the best values obtained for the unvoided and voided (except control subassemblies) $-Tdk/dT \times 10^4$ are (41.21, 12.53, 4.92, 3.07, 6.55, 68.28)[a,b] and (24.86, 7.64, 3.80, 2.57, 5.68, 44.55),[a] and the latter inner-core value reduces by 20% when control subassemblies are also voided. Over the range 1100°-2200°K the values are 9 to 15% higher. The inner core Doppler coefficient decreases by about 3% if the axial and the radial reflectors are reduced to 1/4 and 1/2 of their thicknesses.

c. Sodium void reactivity: Studies have been made of the distribution of sodium void reactivity and its resonance self-shielding part and of the effects of steel and sodium content on sodium void reactivity. From the results of diffusion theory perturbation calculations for adding sodium to the voided reactor and voiding sodium from a normal reactor, and of some k_{eff} differences, the void $\Delta k \times 10^3$ obtained is (11.55, -2.70, -1.45, -0.92, -1.79, 4.69)[b] at a uniform fuel temperature of 1100°K compared to (9.89, -3.03, -0.91, -0.84, -1.53, 3.58) reported in the CRBR PSAR (Table 4.3-10). For the inner core the self-shielding accounts for 16%. The inner core void worth changes by only 6% with steel content changing from 0.5 to 1.5 of normal. The inner core specific worth is found to be constant within 5% with the sodium content changing from normal to zero.

d. Steel worth: Studies have been made of the steel worth distribution and the effects of steel and sodium contents on this distribution. The worth $\times 10^3$ of half of the normal steel with the inner core voided (only about 60% of the total steel is in the cladding) obtained by studying a number

---

[a] Comparison with the PSAR is fairly good.

[b] (inner core, outer core, lower axial blanket, upper axial blanket, radial blanket, total)

of k_{eff} differences and perturbation calculations is (-17.90, -1.05, 1.18, 0.83, 2.09, -14.85). The corresponding distribution agrees with the PSAR (Table D4-18) within 8%. These calculations were done with the inner core voided because in loss-of-flow analysis for CRBR clad relocation is expected to occur after the inner core has almost fully voided.[5] The inner core value increases by about 2% for normal sodium content. The inner core specific worth changes by less than 5% when the steel content changes from 0.5 to 1.5 of normal.

e. Core fuel worth: The distribution of core fuel worth × 10^3 in core and axial blanket regions with the inner core voided is found to be (262.8, 187.8, 39.91, 29.83, 5.94,[c] 526.3). The core total is nearly 6% higher than that reported in the PSAR (Table D4-16). The worth of the core fuel in the axial blankets is needed because in HCDA analysis only core fuel may relocate. The specific fuel worth is highly dependent on the fuel content itself (unlike specific worths of sodium or steel), being lower at higher fuel content. The axial skewness of Doppler coefficients, sodium void, and steel worth distributions each ranges up to 100% and that of core fuel worth from 22 to 37% due mainly to the partial insertion of the control rods.

B. Model Studies

1. Stability of Boiling Fuel/Steel Pools (P. B. Abramson)

A simple energy balance following the basic Hicks-Menzies concept was performed for mixtures of fuel and steel with various mass ratios and initial temperature differences.

Fig. 1 shows the total vapor pressure available from a fuel/steel mixture with equal amounts of fuel and steel with the fuel initially at 3500°K mixed with colder steel. Following each curve from right to left indicates the total pressure rise available in the mixture as heat transfer takes place. Some of the curves show a negative initial pressure response while some show a positive response. Those with positive response have the potential for a stable response to compression if the heat transfer rates are high enough and if the total compressive pressure can be produced by the mixture. Many sets of curves were generated and used to generate Figs. 2 and 3 which are the basic stability criteria for such mixtures.

Fig. 2 shows the maximum temperature difference between fuel and steel which can provide positive response to compression--as functions of mass ratio and fuel temperature at onset of compression.

Fig. 3 is a plot of the maximum pressure rise available from a specific element of fuel/steel mix.

2. Modifications to the POOL Program (P. B. Abramson)

a. Graphics: POOL was modified to use ANL's new FR80 film plotter. A two-minute 16mm demonstration film was made which showed the influence of heat transfer on the response of a POOL to uniform overpressures. For one of the

---

[c] Radial blanket fuel in radial blanket.

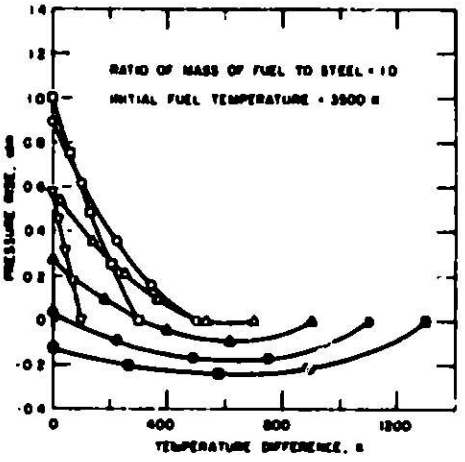

Fig. 1. Fuel/Steel Mixture Pressure Response to Thermal Equilibration. ANL Neg. No. 116-75-212

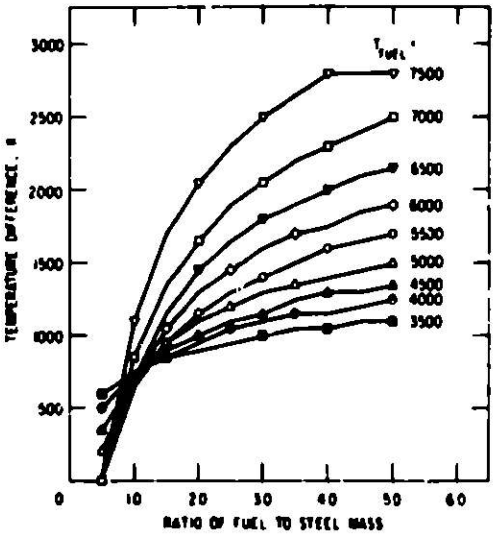

Fig. 2. Maximum Temperature Difference for Stable Response. ANL Neg. No. 116-75-210

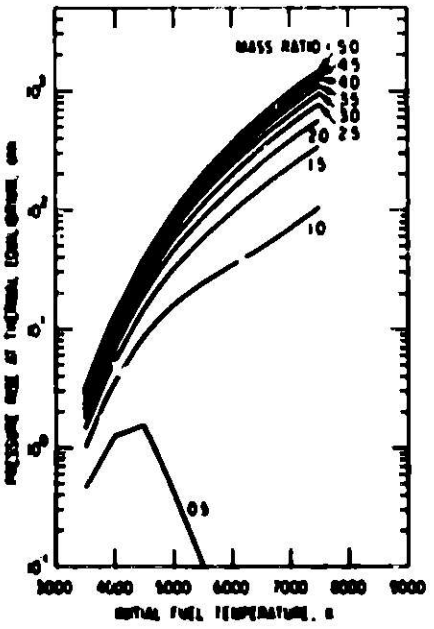

Fig. 3. Maximum Pressure Rise for Fuel/ Steel Mixture. ANL Neg. No. 116-75-209

cases shown the heat transfer rate was high enough that the pool could counter the overpressure by its own internal pressures generated without additional neutronic energy. Two other cases were filmed (created) for which the heat transfer rate was not high enough to allow the internal pressure to respond fast enough to prevent collapse, so that the pool went prompt critical and disassembled by the fuel vapor pressure generated by added neutronic heating. Fig. 4 shows the first case after overcoming the overpressure and Fig. 5 shows the typical result of a neutronic burst. In both cases the new version of POOL which has 6400 marker particles was used.

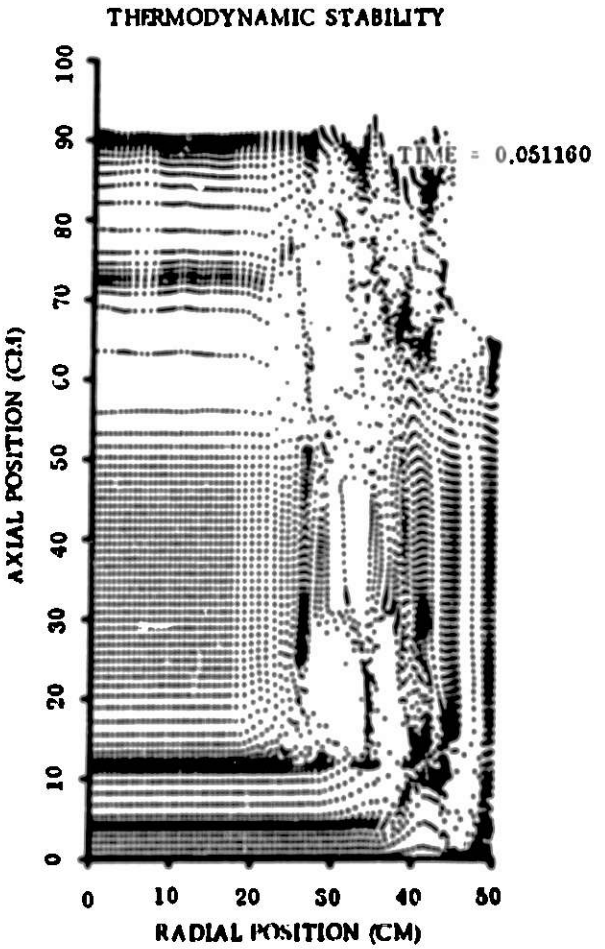

Fig. 4. High Heat Transfer Rates. ANL Neg. No. 116-76-27

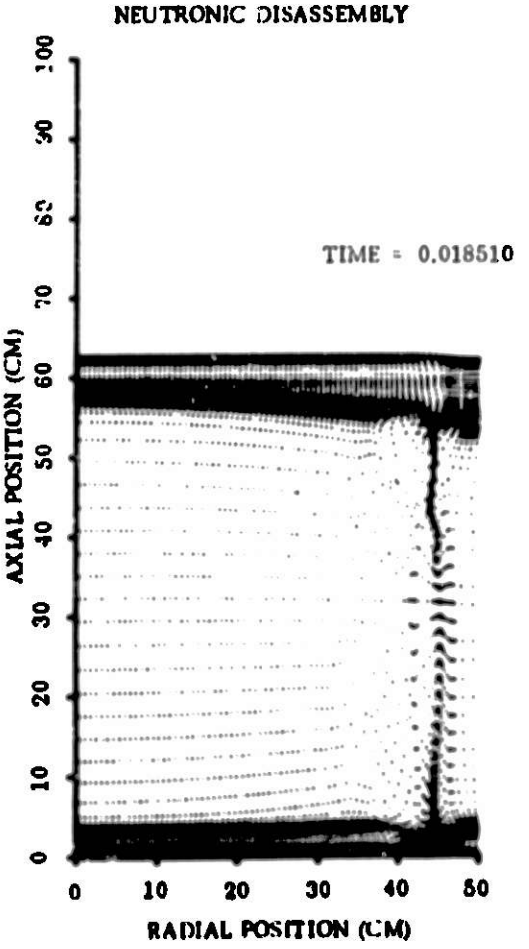

Fig. 5. Low Heat Transfer Rates. ANL Neg. No. 116-76-26

b. Incompressible Regions: Because of our desire to follow long term post-CDA (core disruptive accident) motions and to look for recriticalities, we are attempting to develop a new numerical hydrodynamics technique that combines separate treatments of the compressible and incompressible regions of the pool. At this point, we are trying a combination of the incompressible flow algorithm of Hirt, Nichols, and Romero[6] and the PIC (particle-in-cell) treatment of Harlow and Evans.[7]

The basis of our concept is that one seems to be able to treat the entire region by examining each cell to see if it is incompressible or not. If it is compressible, we intend to use our current POOL algorithms; if incompressible, we are using the modification described below.

The standard technique for dealing with non-satisfaction of the continuity condition in compressible flow calculations of incompressible cells has been to adjust the cell pressure to a higher level until the continuity equation is satisfied when the new velocities predicted from the use of the new higher pressure in the momentum equation are used. This is a time consuming iterative procedure.

Both Hirt et al[6] and earlier Amsden and Harlow[8] suggested that treatment of the over-densification problem in incompressible flows could be solved in primitive variables. Hirt et al use the primitive variables and derive a pressure increment necessary to satisfy both velocity transport and continuity. For those cells which are incompressible we have taken that increment, bypassed (through direct substitution in the momentum equation) the use of an artificial pressure rise and simply used the proper artificial velocity increment in the continuity equation and in the overall iteration scheme. While the technique appears to work, it is not free from problems and we are not, at this point, able to state conclusively its applicability.

In r-z geometry, for non-bounding cells, the algorithm of Hirt et al and Amsden and Harlow may be combined and reduced to the following mathematical form (for interior cells)

$$\Delta U_R = \frac{\Delta V}{2\Delta R V \Delta t} \left(\frac{1}{\frac{1}{\Delta R}^2 + \frac{1}{\Delta Z}^2} \right) \tag{1}$$

and

$$\Delta U_Z = K \frac{\Delta R \Delta U_R}{\Delta Z} \tag{2}$$

where:

ΔV is the excess volume of incompressible fluid introduced into the cell by the velocity field present at the beginning of the time step,

V is cell volume

ΔR is cell radial dimension

ΔZ is cell axial dimension

Δt is time increment

ΔU_R, ΔU_Z are the increments in U_R, U_Z necessary to satisfy continuity,

K is a constant which varies for boundary cells and is 1 for interior cells (per the Hirt algorithm) and thus guarantees zero vorticity and hence zero change in vorticity.

Problems have been encountered to date with both convergence and stability as well as some minor boundary conditions problems. None appear insurmountable.

3. Improved FCI (Fuel-Coolant Interaction) Model
(P. Pizzica)

Debugging of the program for improved treatment of fuel failure with liquid sodium present continued. The transient calculation was carried out to 2 msec or 200 time steps. (No attempt has been made as yet to increase time step size, which will be done after the initial stages of the transient). It was thought, however, that the convection of fuel particles in the channel with a continuous distribution of particles which was originally assumed produced somewhat spurious results. Therefore, the transient was not continued any further. It was decided to use a marker particle and cell scheme instead and this will be programmed in the future.

It was determined by trial and error that the type of model which was originally envisioned for ejecting fuel from the pin into the channel, that of computing an actual ejection velocity based on the difference in pressure between the pin and the channel, is not practical. It predicts far too high ejection rates. This problem could possibly be solved if some orificing factor were included but, since it is impossible to know even approximately what the orifice is, this amounts to an arbitrary and unjustifiable procedure. Perhaps in different circumstances this method could be used; i.e., when the pressure difference is less. But for the time being it has been decided to return to the pressure equilibration model, which assumes that, during one time step, that amount of fuel/fission gas froth will be ejected which is necessary to raise the channel pressure in the node adjacent to the failure node in the pin (and drop the pressure in the pin node which has failed) to some equilibrated value. It was originally thought that an iterative process such as the one described in PLUTO[9] would be necessary. However, after inspection of the equations, it was found that all the requirements of the system could be reduced to one rather complicated cubic equation, eliminating any need for an iterative procedure. After some preliminary debugging, it was found that this method worked satisfactorily in the conditions created by the code thus far. The finite difference techniques used (donor cell) seem to work well so far. However, the most difficult conditions for its testing have not been achieved thus far, that is, conditions occurring in the coolant channel during the advanced stages of an FCI. Many other of the most basic aspects of the model have been debugged and are working well. However, continued progress must wait on the introduction of the marker particle and cell method. As far as the transient was carried out, there is general agreement with the PLUTO code, although modelling differences created some inevitable differences in results.

After the marker particle model is included, voiding into a partially voided channel as well as multi-node failures will be attempted. Then a sodium liquid film calculation will be developed along with a treatment of fuel vapor in the channel, additional fuel melting in the pin, and fission heating of all fuel.

IV. COORDINATION OF RSR SAFETY ANALYSIS RESEARCH

Discussions were held with R. Coats, B. Butcher, and D. Benson of Sandia regarding their first few data points for the vapor pressure of UO_2. Their data appears to be roughly a factor of 5 higher (in pressure) than the ANL VENUS Equation-of-State would predict.[10] For preliminary data it seems good, and the Sandia people expect to generate more data the next time they can get on the equipment (late winter or early spring 1976).

Discussions concerning the RSR ACPR program were held between H. Hummel and T. Schmidt of Sandia at the San Francisco ANS meeting. Contacts were made with Reimar Fröhlich and Ulrich Müller of Germany regarding potential mutual interest in studying recriticality in fast breeder reactors.

Kalimullah visited BNL on Dec. 17 to discuss the calculation of physics parameters needed for CRBR safety studies with Licensing and BNL personnel. He also discussed use of the DEMO code with D. Albright and the status of the SSC code, particularly development of the primary loop model, with A. Agrawal and I. Madine of BNL.

H. Hummel attended a meeting of the ART (Aerosol Release and Transport) Committee in Bethesda on October 30, 1976.

V. EVALUATION OF PROGRESS IN REACTOR SAFETY RESEARCH

Papers presented at Albuquerque PAHR meeting.

"Parameters Influencing Recriticality in Post-CDA Circumstances,"
P. B. Abramson

"Status of Accident Analysis for Fast Breeder Reactors,"
H. H. Hummel

Papers presented at San Francisco ANS meeting.

"Recriticality Studies in Boiling Pools of Fuel and Steel and HCDA Analysis,"
P. B. Abramson

"A Comparison of Three Disassembly Models for a 1000 MWe FBR,"
P. Bleiweis, B. Ganapol, C. Bower, P. Abramson, and D. Weber

"Loss-of-Flow Calculations for the CRBR Demonstration Plant,"
H. H. Hummel, Kalimullah, and P. A. Pizzica

"SYNBURN - A Fast Reactor Fuel Cycle Code,"
P. A. Pizzica and D. A. Maneley

Technical Note
"Basic Stability for Boiling Fuel/Steel Mixtures,"
P. B. Abramson (submitted to Nuclear Science and Engineering)

MONTE CARLO ANALYSIS AND CRITICALS PROGRAM PLANNING FOR SAFETY-RELATED CRITICALS (A2018)

VI. MONTE CARLO ANALYSIS OF SAFETY-RELATED CRITICALS

A. Status of Work on ZPR-3 Assembly 27 (E. M. Gelbard)

The Monte Carlo studies of ZPR-3/27 and ZPR-3/28 have now been completed. For ZPR-3/27 we find,

1. Using ENDF-B/III,
   k=1.001 ± 0.002.
2. Wit
2. With ENDF-B/IV,
   k=1.005 ± 0.002.

3. With ENDF-B/III and the ^{235}U density raised by 1.5%,
   k=1.007 ± 0.003.

Case 3, above, was run because the net ^{235}U inventory reported at the time of the experiment, was 1.5% higher than the inventory completed by VIM from the problem input.

For ZPR-3/28, using ENDF-B/IV, we get k=0.992 ± 0.002. In this case the reported ^{235}U inventory was about 3% higher than that computed by VIM; there seems to be little reason to run or correspondingly adjusted VIM. Generally, the agreement between Monte Carlo and experiment is fairly good, but there is a substantial (1.3%) eigenvalue shift in going from Assembly 27 to 28. This shift is far outside the quoted confidence intervals (which are, in all cases, standard deviations) and would be important if it could be taken seriously. Unfortunately, however, uncertainties in the experimental configuration completely obscure the significance of this shift.

All computations reported above were run with about 100,000 histories, at about 1 minute net computing time per thousand histories.

Monte Carlo calculations in support of the preanalysis of future DEMO safety-related experiments are now in progress. These Monte Carlo calculations will check the validity of multigroup diffusion computations involved in the design and analysis of the proposed experiments. A VIM calculation has already been run for Step 1 in the proposed experimental sequence. The VIM configuration corresponded exactly in geometry and composition, with the configuration of a R-Z diffusion theory design calculation, previously run. The VIM eigenvalue for this case is 0.998 ± 0.002, while the diffusion theory eigenvalue was 1.000.

Step 1 is the experimental sequence represents an undamaged core. Future configurations for badly damaged cores will provide us with more severe tests of conventional diffusion theory methods.

VII. PLANNING OF DEMO SAFETY RELATED EXPERIMENTS

The results of core design scoping calculations for a number of alternate reactor compositions are included in this report. A set of general criteria for the core design was discussed in some detail in the previous quarterly report. The criteria were concerned with core configuration, core composition, core geometry, unit-cell design, mid-plane symmetry, number of configurations in a sequence and the reference meltdown configuration. These criteria have been used in the evaluation of the different compositions and designs. One design was selected for use as the reference design for additional program planning.

A. Core Design Compositions and Scoping Calculations

Five alternate compositions for the base reference core have been defined and analyzed. In addition, three possible high-fuel-density meltdown compositions were studied. Each of these compositions corresponded to a specific critical assembly plate loading (see Fig. 6). Calculations were made for each composition for both bare and reflected homogeneous spherical models using the SDX code. These results are summarized in Table I. The purpose of this work was to select a composition for the reference core. Compositions 1, 2, and 4 were found to be somewhat too reactive -- resulting in cores that were too small. Compositions 3 and 5 were selected for further analysis.

B. Reference Design

Two reference core configurations with height-to-diameter ratios, H/D, of 1.0 and 0.5 were considered for both Compositions 3 and 5. Calculated design parameters for these four possible core designs are summarized in Table II. Based on the criteria stated above, the design in the first column, i.e., the design based on Composition 3 with an H/D of 1.0, is the preferred design and will be used as the reference for purposes of additional program planning. This design has a clean, simple core and blanket configuration with a single-drawer unit cell. The core size is small enough so that leakage effects are emphasized in order to provide an adequate test of the Monte Carlo analysis, however, it is large enough so that the composition is generally representative of current LMFBR designs. Both the enrichment and the ^{239}Pu atom density for this design are intermediate to the CRBR inner and outer core compositions. Of these four core designs included in Table II, only the design selected has both a single-drawer unit cell loading and a core height that is typical of LMFBR design. The differences among these designs are not large however.

C. Meltdown Analysis for Reference Design

Calculations were made for a series of five cores which represent various stages in an idealized meltdown accident. The reference configuration was an undamaged core of Composition 3 with an H/D = 1.0. This reference 2-D cylindrical model is shown as Step 1 in Figs. 7 and 8.

The critical core radius is 46.18 cm. which corresponds to a fissile mass (^{239}Pu + ^{241}Pu) of 368.93 kg. In Step 2 sodium was removed from the central radial region of the core and axial blanket. Two cases were chosen which corresponded to voiding the sodium from: 1) the central 25 drawers, and 2) the

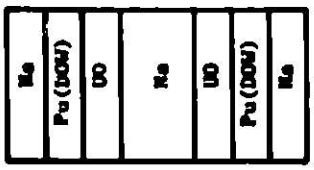

UNIT CELL 1

UNIT CELL 2

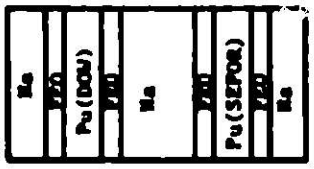

UNIT CELL 3

UNIT CELL 3A

UNIT CELL 3B

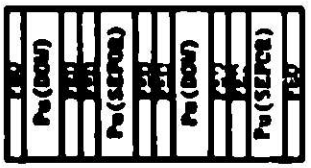

UNIT CELL 3C

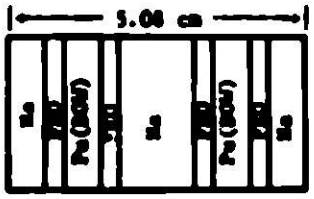

UNIT CELL 4

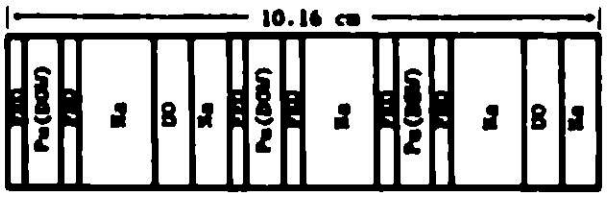

UNIT CELL 5 (TWO QUARTERS)

KEY:

UO = U_3O_8 Plate

Na = Na Can

PEO = Fe_3C_1 Plate

Pu (DOW) = Pu/U/Na CAN (.282/.691/.025, $^{239}Pu/Pu$ = 0.907)

Pu(SEFOR) = Pu/U/Na CAN (.195/.779/.026, $^{239}Pu/Pu$ = 0.940)

Fig. 6. Unit Cell Plate Loadings.

TABLE I. Safety Related Critical Assembly Planning, Reference Core Design Studies

Composition	1	2	3	3a	3b	3c	4	5
				Bare Homogeneous Spherical Models				
Critical Buckling	0.0027882	0.0028991	0.0021743	0.0046347	0.0037870	0.0067263	0.0028787	0.0018417
k_∞ ($B^2 = 0.0$)				1.68839	1.59388	1.71750		1.43601
Critical Radius, cm	59.50	58.75	67.37	66.15	51.05	38.31	58.55	73.21
Volume, ℓ	622.2	849.6	1281.0	411.6	557.3	235.4	840.9	1643.3
Fissile Pu, kg	632.0	698.7	763.9	392.9	490.0	280.0	602.4	882.9
^{239}Pu Density - 10^{22}	1.779	1.779	1.486	2.376	2.082	2.972	1.779	1.335
Enrichment, $\frac{\text{Fissile}}{\text{Heavy Metal}}$	0.1651	0.2007	0.2214	0.2334	0.2092	0.2214	0.2564	0.1872
				Reflected Homogeneous Spherical Models				
Reflector Savings, cm		14.33	15.90	11.52	12.06	9.42		15.69
Core Radius, cm		44.42	51.78	34.63	38.99	28.89		57.52
Core Volume, ℓ		367.0	581.4	173.9	248.3	101.0		797.2
Fissile Pu, kg		263.0	346.7	166.0	207.2	120.4		428.3

TABLE II. Reference Configurations for Meltdown Critical

Composition	Unit Cell No. 3		Unit Cell No. 5	
Core Dimensions				
H/D	1.0	0.5	1.0	0.5
Radius, cm	46.1764	60.7161	51.3847	67.7738
Height, cm	92.3528	60.7161	102.7694	67.7738
Volume, ℓ	618.643	703.172	852.474	977.992
Fissile Pu, kg	368.93	419.34	458.03	525.47
Blanket Dimensions				
Radius, cm	86.1764	100.7161	91.3847	107.7738
Height, cm	172.3528	140.7161	182.7694	147.7738
Volume, ℓ	3402.457	3781.095	3942.655	4414.304

central 37 drawers of the ZPR matrix. In the cylindrical models these regions correspond to radii of 15.58 cm. and 18.96 cm., respectively. In Steps 3 and 4, the fuel within these regions was slumped to one-half the core height and the axial blanket was "dropped" adjacent to the slumped fuel. In Step 5 the radius of the core/radial blanket interface was reduced to produce a critical configuration. All other region boundaries remained the same. The reactivity changes corresponding to each step of these idealized meltdown sequences are summarized in Table III. Also included are the final fissile loadings and region boundaries for each sequence. Table IV shows a comparison of reaction rates and ratios at the reactor center for Steps 1 and 5 for sequence (2) R_c = 18.96 cm. Significant (and measurable) changes occur in these reaction rates and ratios. The threshold fission ratios increase by 20-30% (relative to Step 1). These effects result predominantly from the spectral changes. The real and adjoint broad-group spectra are shown in Figs. 9 and 10. There is approximately 25% more flux above 500 keV in the Step 5 configuration compared to the reference.

Additional design parameters, including reaction rate traverses, central and axial traverse material worths, and Doppler worth, will be calculated using these two-dimensional models of the clean reference core and cores in various stages of a meltdown accident. VIM Monte Carlo analyses are being used for subset of these configurations. This work is currently in progress. Results of these analyses will be included in the next quarterly.

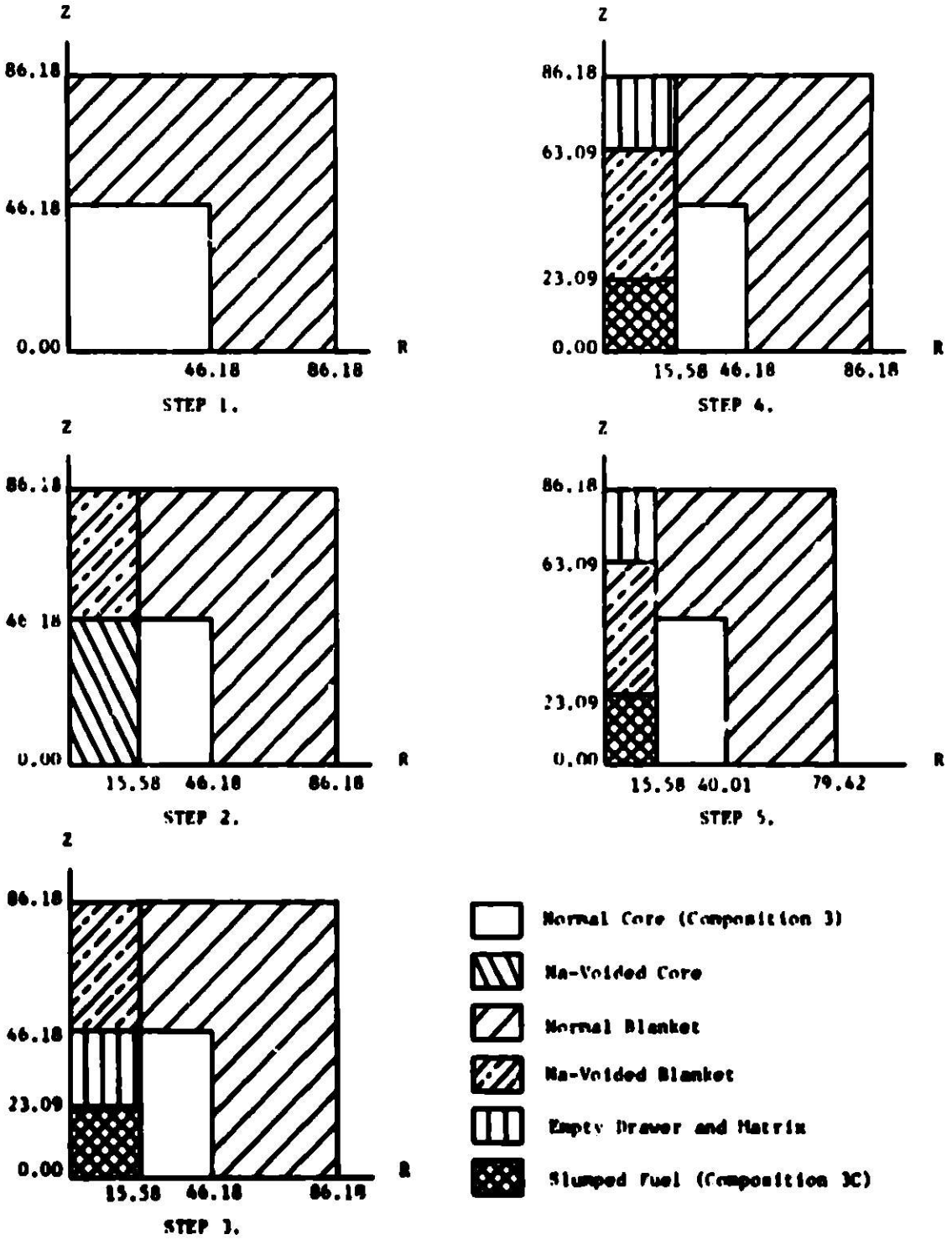

Fig. 7. Two-Dimensional (R-Z) Models for HCDA Sequence. 25 Drawer Slump Zone

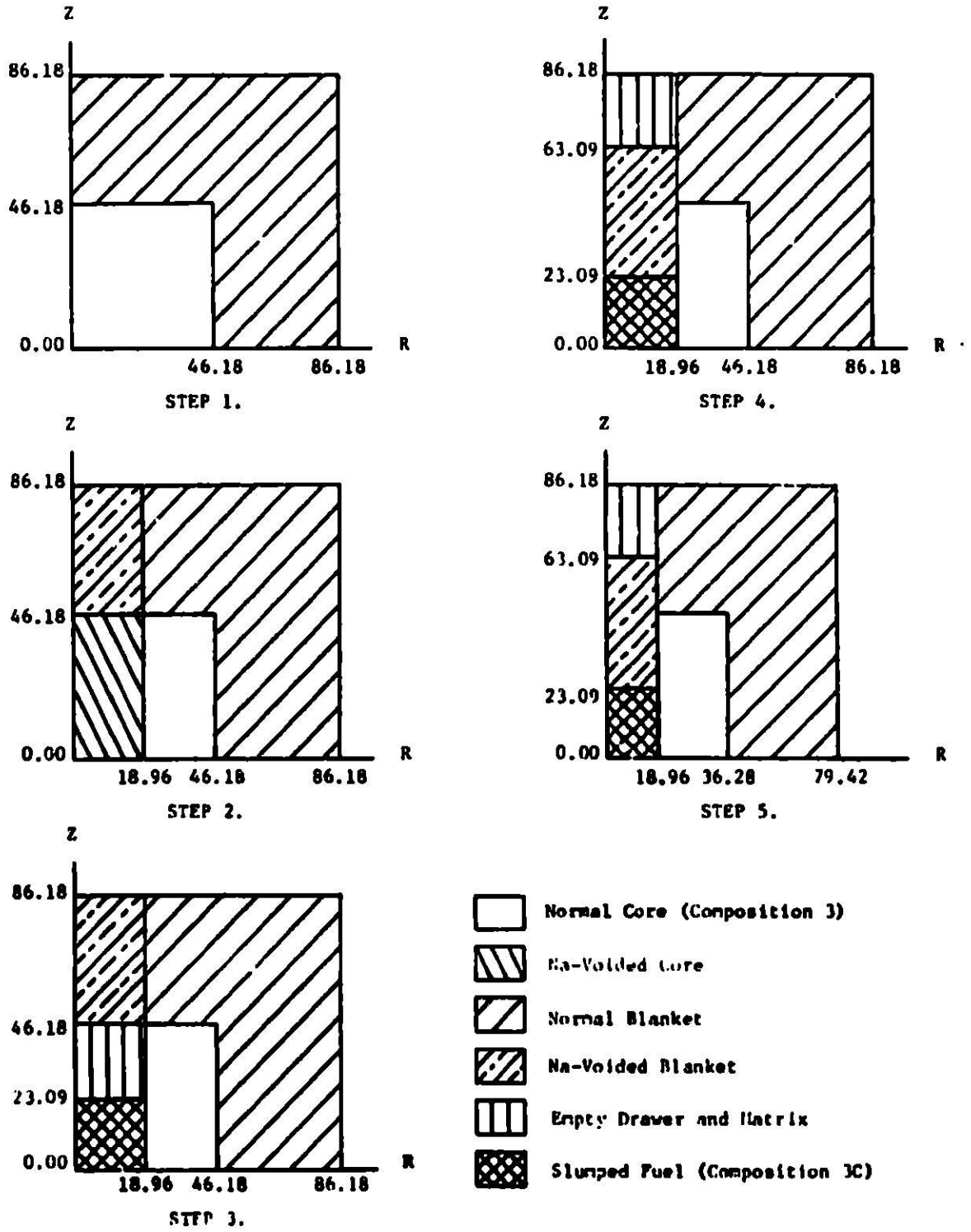

Fig. 8. Two-Dimensional (R-Z) Models for HCDA Sequence. 37 Drawer Slump Zone.

TABLE III. HCDA Sequence for Unit Cell Composition No. 3

		Region of HCDA Sequence	
		(i) 25 Drawers R_a = 15.5843 cm	(ii) 37 Drawers R_a = 18.9592 cm
Step 1.	Reference Configuration R_{core} = 46.18 cm $R_{Blanket}$ = 86.18 cm, H/D = 1.0	k = 1.0000 Fissile Pu = 368.93 kg	k = 1.0000 Fissile Pu = 368.93 kg
Step 2.	Void Na for $r \leq R_a$, $Z \leq 86.18$ cm.	k = 0.9997	k = 0.9993
Step 3.	Slump Fuel for $r \leq R_a$, $Z \leq 23.09$ cm.	k = 1.0323	k = 1.0503
Step 4.	Slump Axial Blanket for $r \leq R_a$, 23.09 cm $\leq Z \leq$ 63.09 cm	k = 1.0448	k = 1.0672
Step 5.	Adjust Core/Radial Blanket Interface to Critical	k = 1.0000 R_{core} = 40.0128 cm $R_{Blanket}$ = 86.18 cm Fissile Pu = 277.01 kg	k = 1.0000 R_{core} = 36.2837 cm $R_{Blanket}$ = 86.18 cm Fissile Pu = 227.79 kg

TABLE IV. Comparison of Reaction Rates and Ratios at Core Center for the Step (Reference) and the Step 5 (Slumped Fuel) Configurations

	$\sum_i \sigma_i^1 \phi_i^1$	$\sum_i \sigma_i^1 \phi_i^5$	$\sum_i \sigma_i^5 \phi_i^5$	$\frac{\sum_i \sigma_i^5 \phi_i^5}{\sum_i \sigma_i^1 \phi_i^1}$
f^{25}	1.72284	1.53281	1.53190	0.88917
f^{28}	5.22159^{-2}	6.57890^{-2}	6.58623^{-2}	1.26135
f^{49}	1.72328	1.66275	1.66258	0.96478
f^{40}	4.35319^{-1}	5.11079^{-1}	5.13351^{-1}	1.17925
f^{41}	2.23980	2.00395	2.00199	0.89383
c^{28}	2.37118^{-1}	1.96007^{-1}	1.92698^{-1}	0.81267
c^{49}	3.75646^{-1}	2.65666^{-1}	2.62826^{-1}	0.69966
f^{25}/f^{49}	0.99974	0.92185	0.92140	0.92163
f^{28}/f^{49}	0.030300	0.039566	0.039615	1.30740
f^{49}/f^{49}	1.0	1.0	1.0	1.0
f^{40}/f^{49}	0.25261	0.30737	0.30877	1.22231
f^{41}/f^{49}	1.29973	1.20520	1.20415	0.92646
c^{28}/f^{49}	0.13760	0.11788	0.11590	0.84234
c^{49}/f^{49}	0.21798	0.15978	0.15808	0.72521

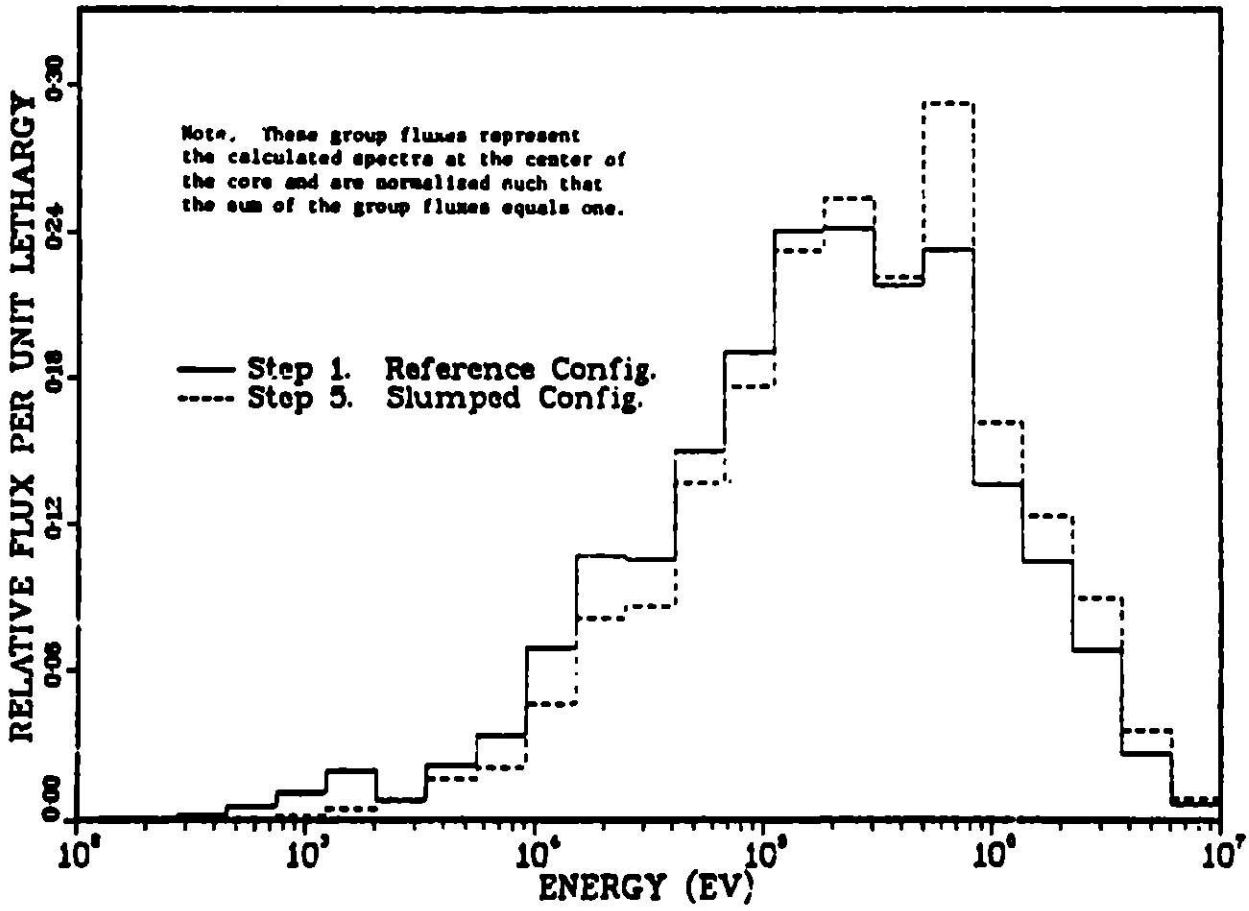

Fig. 9. Broad Group Real Flux at Core Center for Composition 3.

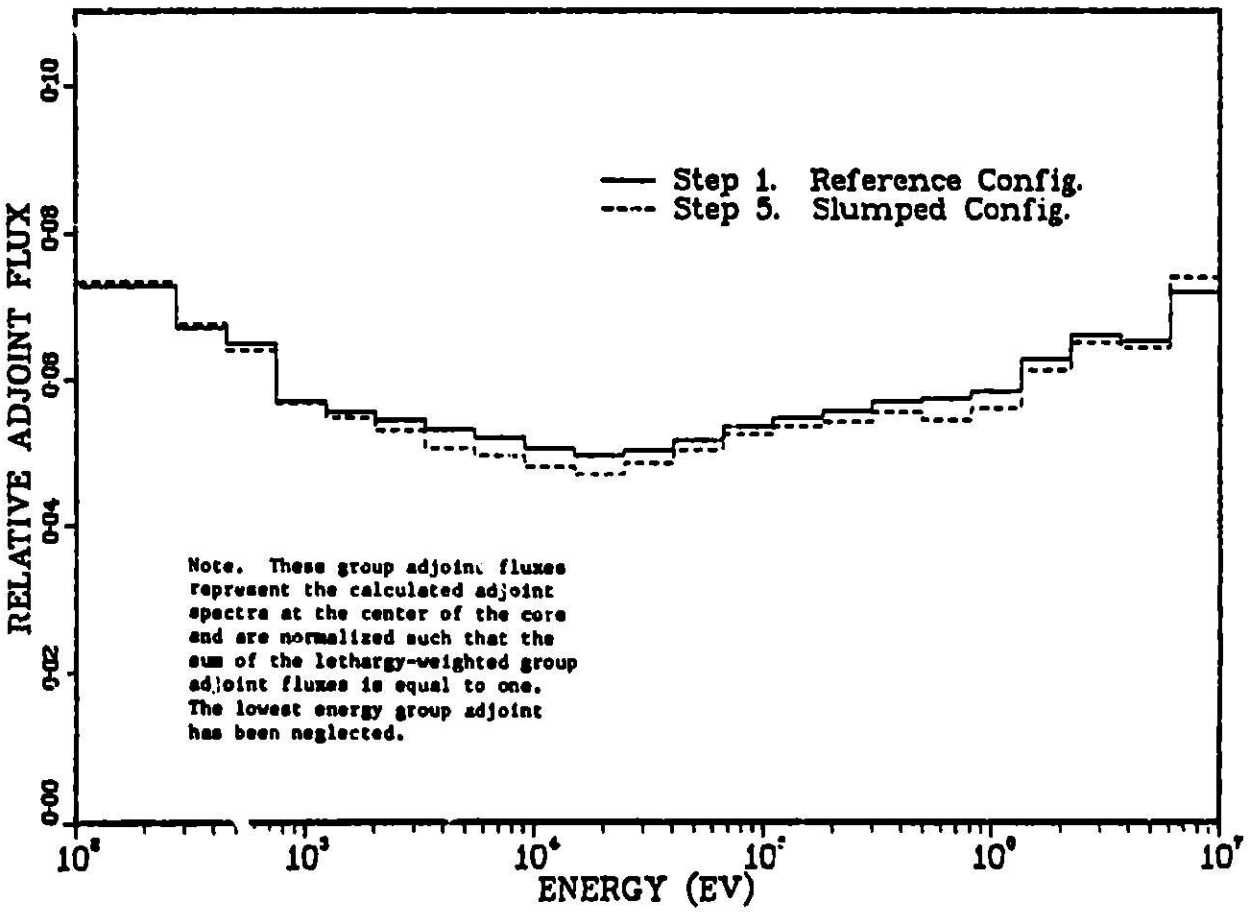

Fig. 10. Broad Group Adjoint Flux at Core Center for Composition 3.

REFERENCES

1. Clinch River Breeder Reactor Plant, Preliminary Safety Analysis Report, Project Management Corporation.

2. F. E. Dunn, et al, "The SAS-2A LMFBR Accident Analysis Computer Code," ANL-8138, Argonne National Laboratory. (October 1974)

3. B. J. Toppel, H. Henryson II, "Methodology and Application of the MC^2-2/SDX Cross-Section Capability," Trans. Am. Nucl. Soc., 16, 126. (1973)

4. W. M. Stacey, Jr., et al, "A New Space-Dependent Fast Neutron Multigroup Cross-Section Preparation Capability, Trans. Am. Nucl. Soc., 15, 292. (1972)

5. H. H. Hummel and P. A. Pizzica, Preliminary Report on Loss-of-Flow Calculations for the CRBR Demonstration Plant, Argonne National Laboratory, RSA-TM-1. (November 1974)

6. C. W. Hirt, B. D. Nichols, and N. C. Romero, "SOLA, A Numerical Solution Algorithm for Transient Fluid Flows," LA-5852, April 1975.

7. M. W. Evans and F. H. Harlow, "The Particle-in-Cell Method for Hydrodynamic Calculations," LA-2139 (1957).

8. A. A. Amsden and F. H. Harlow, "The SMAC Method: A Numerical Technique for Calculating Incompressible Fluid Flows," LASL, May 1970.

9. H. U. Wider, "An Improved Analysis of Fuel Motion During an Overpower Excursion," Ph.D. Thesis, Northwestern University, pp. 47-48, June 1974.

10. J. F. Jackson and R. B. Nicholson, "VENUS-II, an LMFBR Disassembly Program," ANL-7951 (September 1972).